Journal of Applied Remote Sensing

RemoteSensing.SPIEDigitalLibrary.org

Spatio-temporal evaluation of plant height in corn via unmanned aerial systems

Sebastian Varela
Yared Assefa
P. V. Vara Prasad
Nahuel R. Peralta
Terry W. Griffin
Ajay Sharda
Allison Ferguson
Ignacio A. Ciampitti

SPIE.

Sebastian Varela, Yared Assefa, P. V. Vara Prasad, Nahuel R. Peralta, Terry W. Griffin, Ajay Sharda, Allison Ferguson, Ignacio A. Ciampitti, "Spatio-temporal evaluation of plant height in corn via unmanned aerial systems," *J. Appl. Remote Sens.* **11**(3), 036013 (2017), doi: 10.1117/1.JRS.11.036013.

Spatio-temporal evaluation of plant height in corn via unmanned aerial systems

Sebastian Varela,[a] Yared Assefa,[a] P. V. Vara Prasad,[a] Nahuel R. Peralta,[b] Terry W. Griffin,[c] Ajay Sharda,[d] Allison Ferguson,[e] and Ignacio A. Ciampitti[a,*]

[a]Kansas State University, Department of Agronomy, Manhattan, Kansas, United States
[b]Monsanto Argentina, Department of Technology and Development of Corn and Sorghum, Pergamino, Argentina
[c]Kansas State University, Department of Agricultural Economics, Manhattan, Kansas, United States
[d]Kansas State University, Biological and Agricultural Engineering Department, Manhattan, Kansas, United States
[e]PrecisionHawk, Raleigh, North Carolina, United States

Abstract. Detailed spatial and temporal data on plant growth are critical to guide crop management. Conventional methods to determine field plant traits are intensive, time-consuming, expensive, and limited to small areas. The objective of this study was to examine the integration of data collected via unmanned aerial systems (UAS) at critical corn (*Zea mays* L.) developmental stages for plant height and its relation to plant biomass. The main steps followed in this research were (1) workflow development for an ultrahigh resolution crop surface model (CSM) with the goal of determining plant height (CSM-estimated plant height) using data gathered from the UAS missions; (2) validation of CSM-estimated plant height with ground-truthing plant height (measured plant height); and (3) final estimation of plant biomass via integration of CSM-estimated plant height with ground-truthing stem diameter data. Results indicated a correlation between CSM-estimated plant height and ground-truthing plant height data at two weeks prior to flowering and at flowering stage, but high predictability at the later growth stage. Log–log analysis on the temporal data confirmed that these relationships are stable, presenting equal slopes for both crop stages evaluated. Concluding, data collected from low-altitude and with a low-cost sensor could be useful in estimating plant height. [DOI: 10.1117/1.JRS.11.036013]

Keywords: unmanned aerial systems; structure from motion; corn; imagery.

Paper 170039 received Jan. 16, 2017; accepted for publication Jul. 24, 2017; published online Aug. 21, 2017.

1 Introduction

Use of unmanned aerial systems (UAS) to evaluate crop growth, development, and performance is a promising new area of agricultural research.[1–4] Because piloted aircraft and satellite imagery are either prohibitively expensive or not easily available to the required spatio-temporal resolution, the use of UAS has been presented as an alternative.[5] The flexibility of UAS to conduct low-altitude flight and facilitate high-resolution imagery has proven useful for site-specific weed management;[6] to evaluate crop nutrient requirement,[1] soil water status,[7] and crop water stress;[8] and to monitor vegetation growth.[9]

Plant height is one of the major indicators of plant growth and development. Plant height is positively correlated with plant grain yield,[10–12] plant biomass, and soil nitrogen (N) supply.[13,14] Most cereals attain maximum plant height and yield potential at the onset of the reproductive

*Address all correspondence to: Ignacio A. Ciampitti, E-mail: ciampitti@ksu.edu

stage,[15] with approximately half of biomass and N accumulated relative to maturity.[16,17] Therefore, early-season estimation of yield potential in cereals can be generated when the plant attained its maximum height (at flowering) or right before this point (1 or 2 weeks before flowering). Specifically for corn (*Zea mays* L.), plant height is needed for biomass estimation via stem volume calculation (measured via the cylindrical formula based on plant height and stem diameter both determined at comparable phenological stages). Previous researchers documented a high degree of correlation between ground-truthing based stem volume calculation and plant biomass at flowering in corn.[18–24]

Application and process involved in plant height measurement conducted using UAS platforms were discussed by few researchers.[25–27] The process involves (i) collecting aerial data imagery from a camera mounted onboard in UAS, (ii) generating ultrahigh resolution crop surface models (CSMs), and (iii) determining plant height from the CSM,[28] herein, defined as CSM-estimated plant height. However, studies validating CSM-estimated plant height via ground-truthing measurements to predict field crop yields are scarce in the scientific literature.

Early- or even mid-season crop production forecasts assist producers to make informed decisions regarding crop and nutrient management, yield estimation, marketing, storage, and transportation.[29–32] Various models have been used to make such predictions but current applications of most of these models are only for large-scale (regional- or state-level) production systems. As crop management progresses from large-scale uniform management to site-specific using precision agriculture technologies, evaluation of within-field variation and more accurate yield forecasts should be pursued. Following this rationale, plant height relates not only to plant growth during the vegetative stages, but this plant trait can also be used to improve the relationship between active optical sensor readings and yield estimates.[31,32] Therefore, accurate and rapid plant height prediction could facilitate and improve yield forecast in corn. The overall objective of this study was to examine the relationship between plant height data collected from UAS at critical developmental stages and the final biomass estimation of corn hybrids of different maturity groups under different N management and planting densities.

2 Materials and Methods

2.1 *Study Area and Dataset*

During the 2015 growing season, four corn experiments were established in 1.2 hectares at Ashland Bottoms Farm, Manhattan, Kansas (39.13°N, −96.6°E, 314 m above sea level) (Fig. 1).

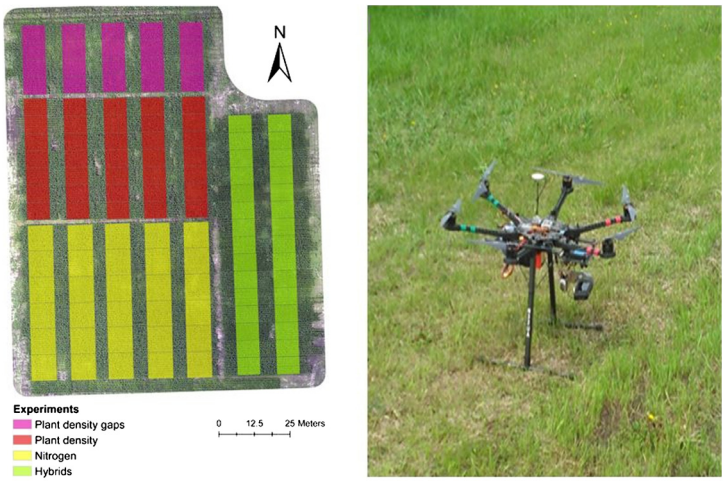

Fig. 1 (a) Study area with four corn experiments evaluating: (i) hybrids, (ii) fertilizer *N* rates, (iii) plant densities, and (iv) plant density gaps and (b) photo of the UAS S800 DJI hexacopter mounted with RGB sensor.

The nitrogen experiment (NE) was implemented in 9.1 m × 10.6 m plots, with five N fertilization levels using urea ammonium-nitrate ranging from 0 to 200 kg N ha^{-1}, in 50 kg N ha^{-1} intervals. The plant density experiment (PE) and plant density gap experiment (PGE) were conducted in 6.1 m × 10.6 m plots, whereas the hybrid experiment (HE) was planted in 6.1 m × 12.2 m plots. All experiments were evaluated in randomized complete block design with five replications. Across all studies, row spacing was 0.76 m. Target plant density was 8.4 plants m^{-2} in NE and HE, and a range between 4.4 and 10.4 plants m^{-2} for the PE and PGE. Corn hybrid used in NE, PE, and PGE was DK61-88 (Dekalb®, Monsanto) 111 days commercial relative maturity (CRM). For the HE, corn hybrids evaluated were DK61-88, DK63-55 (113 CRM), DK64-69 (114 CRM), and P1105 and P1151 (111 CRM; Dupont Pioneer®). All four corn trials were used as a base line to generate spatio-temporal variability of plant height, biomass, and yield to evaluate UAS and structure from motion under different plant height scenarios.

2.2 *Platform, Sensor, and Ground-Truthing*

An UAS platform (S800, DJI, Shenzhen, China) was used to collect aerial imagery. This platform includes the Wookong-M onboard autopilot system and GPS v2 unit (S800, DJI, Shenzhen, China). Flight missions and parameter settings were assigned using UgCS ground station software.[33] The platform sensor included in each flight was Alpha ILCE A5100 RGB Sony (Tokyo, Japan), mounted with a Sony SELP1650 PZ 16-50 mm lens (sensor resolution is 6000 × 4000 pixels). Aperture and exposure time were adjusted manually prior to each flight mission considering the ground speed of the UAS and light conditions at the time of flights. In both flights, camera setting was performed using manual exposure control; shutter speed was set to 1/4000 s, aperture to f5, and ISO to 640 and 16 mm focal length configuration. Two UAS missions were performed (17 and 29 July). Highly visible yellow and black (1 m × 1 m) cross-centered plastic ground targets were used as ground control points (GCPs). In this project, 14 yellow and black cross-centered plastic (1 m × 1 m) GCPs were used as main sources for imagery geolocation. The GCPs were distributed on the borders and internal alleys of the experiments following[34] the recommendations. The average distance between GCPs was 42 m in both missions.

Two critical corn growth stages were identified as target candidates for UAS missions: (1) the late vegetative herein termed as preflowering and (2) onset of reproductive or flowering stage.[35] These UAS mission timings were relevant because of the importance of the aforementioned corn growth stages to determine if plant height estimates can populate crop yield forecasting models. The goal of this step was to overlay CSMs from UAS with ground-truthing data then check goodness-of-fit of CSMs to capture spatio-temporal change of plant height at both stages. The ground-based data collection was divided into destructive biomass sampling and nondestructive *in situ* plant height measurements. GCPs and plant samples were georeferenced by implementing a Global Navigation Satellite System–Real-Time Kinematic survey for spatial and temporal monitoring. The data layer containing the geolocated plant positions was overlaid with the orthomosaic and CSMs using ArcMap (ArcGIS v10.3, Environmental System Research Institute Inc.).[36] Absolute plant height, field ground-truthing, was measured via a centimeter resolution wooden ruler. Field sampling procedures define absolute plant height as the vertical distance between the base of stem and the top region of the plant where leaves reach maximum height without any external intervention ($n = 331$ plants measured 2 weeks before flowering and $n = 331$ plants determined at flowering). Stem diameter ($n = 331$ measured) was determined at the base of the plant following the procedure described by Ciampitti et al.[20] The field measurement performed 2 weeks before flowering was separated by 5 days from the UAS mission; thus plant height was adjusted to the date of the UAS mission using the observed plant height change rate computed between flowering and 2-weeks prior. This adjustment did not modify the proportion of variation accounted for the aerial imagery but significantly reduced the bias in the final observed plant height values, with lower plant height values for the ground-truth data (adjusted by 5 days within the period of height growth). For biomass determination, each individual plant was cut at the stem base and fresh weight was collected *in situ*. Both stem diameter and plant biomass were measured only at flowering time.

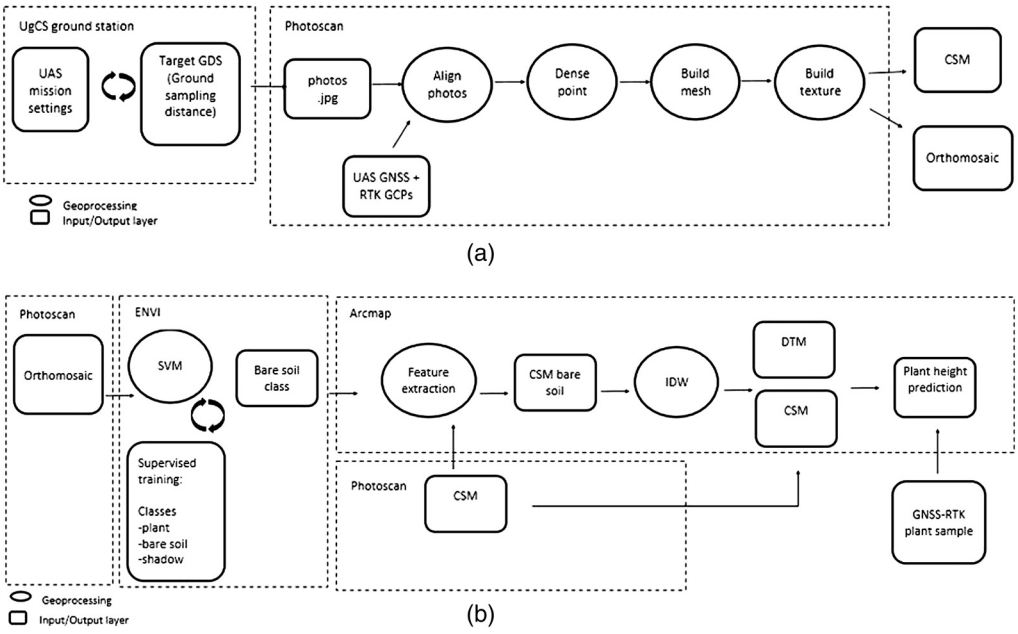

Fig. 2 (a) Workflow data integration between UAS and Photoscan and (b) Photoscan–ENVI–ArcMap data workflow.

2.3 *Data Processing Workflow: Crop Surface Model, Orthomosaic Generation, and Plant Height*

The UAS missions were conducted at 65-m altitude to achieve a ground sampling distance, expressed as the distance between the centers of two consecutive pixels measured on the ground, of 0.015 m. An overlapping and side lapping of 80% was employed in accordance with Photoscan manual recommendations for successful CSM reconstructions [Fig. 2(a)].[37] Ground speed setting of the UAS was 7 ms^{-1} obtaining one image per 1.8 s to achieve the expected overlapping on the track of the UAS. A total of 265 images were collected per mission. The GCPs and UAS imagery data set were integrated and processed for true color [red, green, and blue (RGB)] orthomosaic and CSMs for plant height.

A workflow for CSMs reconstruction was implemented using Photoscan [Fig. 2(a)]. Processing steps included: feature matching, solving camera intrinsic, and extrinsic orientation parameters, reconstructing of the dense point cloud (DPC), and texture mapping. Parameter setting for imagery alignment presented the following characteristics: low accuracy and referenced pair preselection, tie and key points limited to 0 and 40000. The Photoscan imagery aligment algorithm detects points in the source images, which are stable under changing viewpoints and lighting conditions.[37] Then, Photoscan software generates a descriptor for each point based on its local neighborhood. These descriptors are used to detect correspondences across the images.[37] Later the software estimates the camera intrinsic and extrinsic orientation parameters using the internal bundle-adjustment algorithm to approximate accurate camera locations.[37] The distance between all GCPs was comparable and located along the image data set to minimize horizontal and vertical geometrical error. The DPC was reconstructed by Photoscan by implementing the height-field algorithm based on pairwise depth map computation. Moreover, the quality value for the DPC recontruction was set to medium for optimizing the computation time and data set size following Photoscan manual recomendations. The DPC reconstruction achieved 2550 and 2765 points/m^2, respectively, for each mission timing. A spatial interpolation procedure, via inverse distance weighting (IDW), was applied to the DPC to generate the CSM. Orthomosaic and CSM native Photoscan spatial resolutions were 1.0 and 2.0 cm/pixel for data sets from both missions.

The absolute plant height estimation was solved as the difference between the CSM and a digital terrain model (DTM) of bare ground surface [Fig. 2(b)]. The DTM was reconstructed from the flowering RGB orthomosaic (captured 2-weeks prior) and CSM data sets.[26] The first step includes the ground class segmentation in the RGB orthomosaic [Fig. 2(b)]. A support vector machine (SVM) classification was implemented in ENVI[38] to solve the ground class segmentation [Fig. 2(b)]. The training data set included 4000 pixels and iterated in "vegetation," "bare soil," and "shadow" classes. In the iteration phase, a linear discriminant was explored with unsatisfactory results (over all accuracy = 0.55). Thus, a nonlinear classification approach was implemented on the decision surface hyperplane and a radial kernel function was utilized for discrimination between classes. The gamma in kernel function was set to 0.25, the inverse of the number of computed attributes,[39,40] and the penalty parameter was set to 95.[40] The overall accuracy of the nonlinear SVM classification on the three classes was 0.79. The "bare soil" raster was exported from the CSM with bare soil areas into ArcMap and the DTM solved by using the overlapping CSM vertical and horizontal determined from the bare soil over the bare soil class data from segmented ground class regions. Ground class regions utilized in the IDW interpolation included the borders and alleys of the trials, considering an average distance of 12 m between adjacent alleys.

The absolute plant height estimated data were obtained by a map algebra subtraction between the CSM and the DTM over 0.08-m cylinder radius length assigned to each plant center location [Fig. 2(b)]. Estimated plant height was assigned to upper mean quintile CSM pixels in the cylinder area assigned to each plant.

2.4 *Plant Height Validation and its Relationship with Stem Volume and Biomass*

Plant height data extracted from UAS imagery analysis and collected from field measurements (ground-truth data) were linearly regressed using the GraphPad Prism software.[41] The proportion of variation accounted by the fitted model at each developmental stage was evaluated. In addition, a linear relationship between plant biomass and stem volume calculation was examined; whereas an exponential model was fitted for the plant biomass and plant height obtained via CSM. Both fits were performed using the GraphPad Prism software. For plant height validation, model fit was calculated by determination of the root mean square error (RMSE, measurement of estimated versus observed values). Outlier detection was executed via the robust standard deviation of the residuals.[42]

An allometric evaluation was performed for plant height data extracted from UAS imagery and within-field measurements. Thus, reduced major axis was performed with the Standardised Major Axis Estimation and Testing Routines (SMATR) contributed package[43] to R development software.[44] For the different phenological timings, slopes were tested to compare independent fit versus a shared fit for this parameter (if slopes are equal or not). Parameters were $\log_{10}$ transformed ($Y = \alpha X^{\beta} \rightarrow \log\ Y = \log\ \alpha + \beta\ \log\ X$) prior to the analysis[45] and normal distribution of residuals was verified.

3 Result and Discussion

3.1 *Crop Surface Model and Orthomosaic Generation*

Early process of CSM construction is presented in Fig. 3. The UAS images taken at different sections were stitched together using GCPs as a reference (Fig. 3) in PhotoScan software. The importance and the number of GCPs necessary to ensure accuracy of UAS image construction have been previously discussed by other researchers.[46–48]

In terms of geometric quality, the accumulated horizontal and vertical error was 0.7 cm/pixel in orthomosaic and CSM from 2-weeks prior to flowering, and 0.5 cm/pixel for the flowering raster products. Furthermore, a woody table (dimensions = 0.8 m length × 0.4 m wide × 0.6 m height) was used for nonvegetation geometric evaluation. A total of six local GCPs were implemented along the top of the table to evaluate the vertical displacement between the original GCPs and the same one located in the CSM reconstruction. The vertical error in this case was 0.6 cm/pixel.

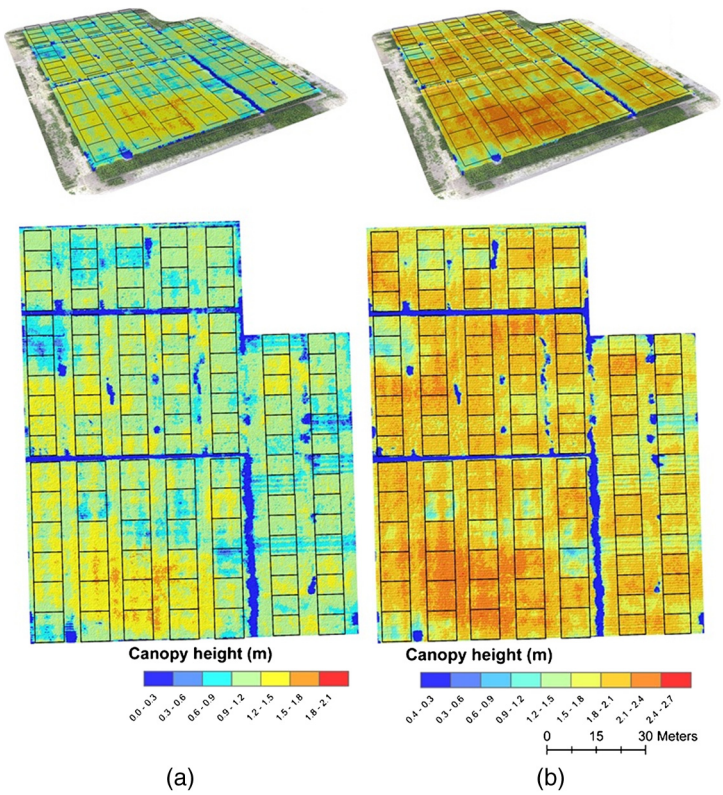

Fig. 3 CSMs for estimated absolute plant height on top of the corn canopy: (a) 2-weeks prior to flowering and (b) flowering time. Upper part: 3-D view and; lower part: 2-D perspectives for corn plant height. Note: The blue color represents ground and low vegetation, the yellow refers to short-medium corn plants, and the brown and red colors represent taller plants within the corn canopy.

3.2 *Plant Height from Unmanned Aerial Systems Versus Ground-Truth Plant Trait*

A strong positive correlation was obtained between CSM-estimated plant height and ground-truth data collected when corn plants were at flowering stage ($R^2 = 0.79$, RMSE = 0.09 m, $n = 331$, and mean = 1.84 m) [Fig. 4(b)]. The correlation between CSM and ground-truth data measured two weeks prior to flowering ($R^2 = 0.63$, RMSE = 0.11 m, $n = 331$, and mean = 1.05 m) was relatively weaker (lower R^2) and with a slightly higher RMSE [Fig. 4(a)]. The RMSE to mean plant height ratio prior to flowering was 14%, close to threefold higher compared to the ratio estimated at flowering time (5%). For the preflowering measurement, the lower proportion of the variation accounted for the CSM-estimated plant height was primarily due to lack of uniform development within the corn canopy and plants emerging at different timing due to soil–weather factors (e.g., saturated soil areas, low residue with less temperature). At flowering, maximum plant height was attained,[49] corn canopy become more uniform with less heterogeneity (lower RMSE to mean plant height ratio) and better prediction power (higher R^2).

A correlation obtained between measured and CSM-estimated plant height is consistent with previous findings for corn,[25,26,50] barley (*Hordeum vulgare* L.), and rice (*Oryza sativa* L.).[27,51] A significant correlation between plant height measurements at flowering stage support the conclusion drawn by Geipel et al.[50] that imagery taken at end of stem elongation is better correlated with ground-truth data. Few researchers have studied the corn growth stage that UAS imagery should be taken to improve plant height estimation.[50,52,53] Other studies not using UAS imagery to evaluate the relationship between actual plant height and remotely sensed plant height[52] also concluded that late vegetative stage sensor-based plant height measurements correlated with actual plant height. Additionally, plant height measurements at late stage of corn were found to correlate with grain yield.[54]

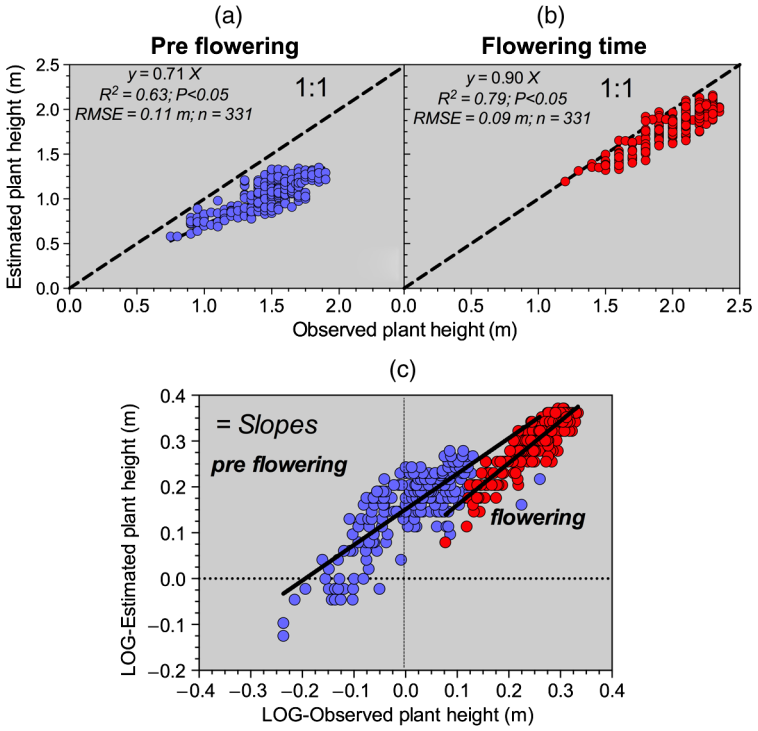

Fig. 4 Plant height estimation via UAS imagery collection (a) 2-weeks prior, (b) at flowering, and (c) log–log linear regression of estimated- to observed-plant height (determined from the ground base to the top of the canopy). RMSE, root mean square error.

It is worth noting that at both corn stages plant height was underestimated, similar to the findings presented by Grenzdörffer[26] and Shi et al.[53] For understanding the stability of the plant height estimation, two evaluations were executed. The first one was done by comparing the linear regression slopes (for equality) of the estimated- and observed-plant height relationship [Figs. 4(a) and 4(b)] between the two growth stages evaluated to understand the stability of the estimation between dates and across plant height class (log–log transformation analysis) [Fig. 4(c)]. Results showed similar slopes across classes for both mission timings. A second evaluation was performed to understand the absolute and relative magnitude of the plant height estimation for both dates. Ground-truth plant height data were divided into three equal classes for each crop stage. Prior flowering ground-truth mean plant height data classes were low 1.22 m, medium 1.52 m, and high 1.71 m. For the 2 weeks before flowering timing, within the low plant height group, 22% of the data in this class were underestimated by the CSM-estimated plant height trait; while for the high plant height group, this analysis resulted in 24% of the plant height observations being underestimated. At flowering, only 10% of the data on plant height across all classes (low 1.77 m, medium 2.12 m, and high 2.24 m) were underestimated by the CSM-estimated plant height trait. Synthesizing, this analysis allowed us to conclude that there was a better prediction of plant height due to a lower underestimation at flowering, which was also related to lower plant heterogeneity within the corn canopy.

3.3 *Unmanned Aerial Systems Based Plant Height Relation with Biomass*

Since ground-truth plant height was better estimated at flowering, the biomass data collected at the same growth stage were utilized to better understand the relationship between plant height and plant biomass. Plant biomass and CSM-estimated plant height exhibited a statistically significant correlation at flowering [Fig. 5(a)]. However for the plant biomass trait, the proportion of the variation accounted by the CSM-estimated parameter alone was low ($R^2 = 0.31$, $n = 332$, and $P < 0.05$). Examination of Fig. 5(a) shows substantial variation present in the data, and possibly nonlinear behavior at greater plant height values. Plant biomass estimation substantially

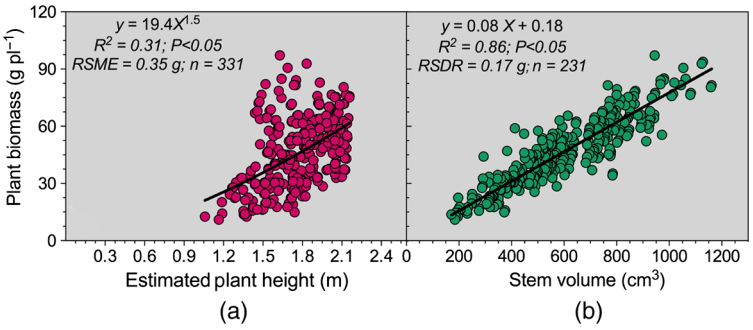

Fig. 5 Per-plant biomass (dry basis, expressed in g pl^{-1}) versus (a) plant height trait estimated via CSM and (b) stem volume estimated via implementation of the volumetric cylinder equation (including plant height estimated via CSM, CSM-estimated plant height) all parameters determined at flowering.

improved ($R^2 = 0.79$, $n = 332$, and $P < 0.05$) when the stem diameter (determined at equal growth stage and for the same plants as the plant height trait) was considered as a part of the stem volume calculation [Fig. 5(b)]. Allometric equations were previously utilized in corn to predict biomass with different levels of success depending on the variation of the data (genotype by environment by management interaction) and the timing of the sampling.[15,55,56] More accurate biomass estimation performed via utilization of allometric models could be utilized as a tool to forecast corn yields. Last, improvements of biomass prediction for corn after flowering stage were documented when the apical ear shoot diameter (maximum diameter of the ear organ) was included in the stem volume calculation.[23] Thus, improvement in corn biomass prediction will be of a great challenge for the remote sensing discipline because the reproductive organs (ears) are placed at varying positions within the corn canopy. In a simplified approach, a combination of various data layers collected from multiple sensors [e.g., plant height, stand counts, normalized difference vegetation index (NDVI)[57]] in a spatio-temporal fashion might allow to adjust in real-time corn yield estimations based not only on plant size but also considering plant nutrient status and the complex interaction with the environment.

For corn crop, a correlation between ground-truth plant height measured at late vegetative or early reproductive and plant biomass has been previously documented.[12,15] For the current study, plant height was adequately predicted for both corn growth stages: 2-weeks before (with more variation detected) and at flowering. Similarly, a significant positive relationship between corn plant height measured late-vegetative using sensors, mounted on satellite or run manually, with biomass or yield was reported.[17,58] Not many UAS based results are available for corn,[50,53] but our results on the relationship between plant height measured by UAS platform with biomass is in agreement with previous research reported for other field crops.[27,51]

Last, the relationship documented in this study for corn crops between stem diameter and plant biomass is in line with findings previously presented by Mourtzinis et al.[15] A nondestructive way of measuring stem diameter from images mounted on UAS and other ground-truth sensors remains as a critical research gap for improving plant biomass prediction and the potential for yield forecasting purposes. From a remote sensing standpoint, different vegetation indices and multi/hyperspectral sensors can be investigated to improve plant biomass prediction and yield forecast procedure.

4 Conclusions

Spatial-temporal correlation between CSM-estimated versus ground-truthing plant height trait suggested that the CSM integration could assist in biomass estimation. Both dates evidence plant height underestimation but with higher departure for this trait for the pre-flowering stage. Imagery overlapping and plant height heterogeneity become critical factors in the plant height estimation process. At flowering stage, plant biomass and yield prediction could still be used for late management practices, such as nutrient fertilization and fungicide/insecticide protection. Nonetheless, accurate corn yield prediction at early growth stage (before flowering) remains

a topic needing additional research. The evidence suggests that both plant traits such as stem diameter and/or nutrient content estimation should be targeted to increasing reliability of forecasting yield procedures. Future research should also look into the integration of UAS and spectral remote sensing data into ultrahigh spatial-resolution analysis for crop growth modeling.

Acknowledgments

The authors are thankful for the support from Kansas State University (Global Food Systems award from the Kansas Department of Commerce), PrecisionHawk, and the Kansas Corn Commission. This is Contribution No. 16-123-J from the Kansas Agricultural Experiment Station.

References

1. E. R. Hunt et al., "Evaluation of digital photography from model aircraft for remote sensing of crop biomass and nitrogen status," *Precis. Agric.* **6**, 359–378 (2005).
2. W. S. Lee et al., "Sensing technologies for precision specialty crop production," *Comput. Electron. Agric.* **74**, 2–33 (2010).
3. J. M. Peña et al., "Weed mapping in early-season maize fields using object based analysis of unmanned aerial vehicle (UAV) images," *PLoS One* **8**(10), e77151 (2013).
4. J. Primicerio et al., "A flexible unmanned aerial vehicle for precision agriculture," *Precis. Agric.* **13**, 517–523 (2012).
5. S. Herwitz et al., "Imaging from an unmanned aerial vehicle: agricultural surveillance and decision support," *Comput. Electron. Agric.* **44**, 49–61 (2004).
6. J. Torres-Sánchez et al., "Configuration and specifications of an unmanned aerial vehicle (UAV) for early site-specific weed management," *PLoS One* **8**, e58210 (2013).
7. S. Ryo, N. Noguchi, and K. Ishii, "Correction of low-altitude thermal images applied to estimating of soil water status," *Biosyst. Eng.* **96**, 301–313 (2007).
8. P. J. Zarco-Tejada et al., "Fluorescence, temperature and narrowband indices acquired from a UAV platform for water stress detection using a micro-hyperspectral imager and a thermal camera," *Remote Sens. Environ.* **117**, 322–337 (2012).
9. J. A. J. Berni et al., "Thermal and narrowband multispectral remote sensing for vegetation monitoring from an unmanned aerial vehicle," *IEEE Trans. Geosci. Remote Sens.* **47**, 722–738 (2009).
10. C. N. Law, J. W. Snape, and A. J. Worland, "The genetic relationship between height and yield in wheat," *Heredity* **40**, 133–151 (1978).
11. D. S. Shrestha et al., "Plant height estimation using two sensing systems," in *ASAE Annual Int. Meeting Proc.*, St. Joseph, Michigan (2002).
12. X. Yin et al., "Comparison of models in assessing relationship of corn yield with plant height measured during early- to mid-season," *J Agric. Sci* **3**, 14–24 (2011).
13. X. H. Yin and M. A. McClure, "Relationship of corn yield, biomass, and leaf nitrogen with normalized difference vegetation index and plant height," *Agron. J.* **105**, 1005–1016 (2013).
14. S. Gul et al., "Effect of sowing methods and NPK levels on growth and yield of rainfed maize (Zea mays L.)," *Scientifica* **2015**, 198575 (2015).
15. S. Mourtzinis et al., "Corn grain and stover yield prediction at R1 growth stage," *Agron. J.* **105**, 1045–1050 (2013).
16. I. A. Ciampitti and T. J. Vyn, "Physiological perspectives of changes over time in maize yield dependency on nitrogen uptake and associated nitrogen efficiencies: a review," *Field Crops Res.* **133**, 48–67 (2012).
17. K. W. Freeman et al., "By-plant prediction of corn forage biomass and nitrogen uptake at various growth stages using remote sensing and plant height," *Agron. J.* **99**, 530–536 (2007).
18. C. A. Miles, "Divergent selection of sweet corn (Zea mays L. var. saccharata) under low and conventional nitrogen environments," PhD Dissertation, Cornell University, Ithaca, New York (1993).

19. L. Borras and M.E. Otegui, "Maize kernel weight response to post flowering source sink ratio," *Crop Sci.* **41**, 1816–1822 (2001).
20. I. A. Ciampitti et al., "Potential physiological frameworks for mid-season field phenotyping of final plant nitrogen uptake, nitrogen use efficiency, and grain yield in maize," *Crop Sci.* **52**, 2728–2742 (2012).
21. K. E. D'Andrea, M. E. Otegui, and A. G. Cirilo, "Kernel number determination differs among maize hybrids in response to nitrogen," *Field Crops Res.* **105**, 228–239 (2008).
22. G. A. Maddonni and M. E. Otegui, "Intra-specific competition in maize: early establishment of hierarchies among plants affects final kernel set," *Field Crops Res.* **85**, 1–13 (2004).
23. E. Pagano and G. A. Maddonni, "Intra-specific competition in maize: early established hierarchies differ in plant growth and biomass partitioning to the ear around silking," *Field Crops Res.* **101**, 306–320 (2007).
24. C. R. C. Vega et al., "Reproductive allometry in soybean, maize and sunflower," *Ann. Bot.* **85**, 461–468 (2000).
25. D. Anthony et al., "On crop height estimation with UAVs," in *IEEE/RSJ Int. Conf. on Intelligent Robots and Systems (IROS 2014)*, Chicago, pp. 4805–4812 (2014).
26. G. J. Grenzdörffer, "Crop height determination with UAS point clouds," in *Int. Archives of the Photogrammetry, Remote Sensing and Spatial Information Science, Volume XL-1, ISPRS Technical Commission I Symp.*, Denver, Colorado (2014).
27. J. Bendig et al., "Combining UAV-based plant height from crop surface models visible and near infrared vegetation indices for biomass monitoring in barley," *Int. J. Appl. Earth Obs. Geoinf.* **39**, 79–87 (2015).
28. J. Bendig, A. Bolten, and G. Bareth, "UAV-based imaging for multi-temporal, very high-resolution crop surface models to monitor crop growth variability," *Photogramm. Fernerkundung Geoinf.* **2013**(6), 551–562 (2013).
29. G. L. Hammer et al., "Advances in application of climate prediction in agriculture," *Agric. Syst.* **70**, 515–553 (2001).
30. N. Kantanantha, N. Serban, and P. Griffin, "Yield and price forecasting for stochastic crop decision planning," *J. Agric. Biol. Environ. Stat.* **15**, 362–380 (2010).
31. D. Franzen, L. K. Sharma, and H. Bu, *Active Optical Sensor Algorithms for Corn Yield Prediction and A Corn Side-Dress Nitrogen Rate Aid*, North Dakota State University, SF1176-5 (2014).
32. W. R. Raun et al., "Optical sensor based algorithm for crop nitrogen fertilization," *Commun. Soil Sci. Plant Anal.* **36**, 2759–2781 (2005).
33. SPH, "UGCS Software for mission planning and execution for all types of unmanned vehicles," SPH Engineering, 2013, https://www.ugcs.com/en/page/products (26 November 2016).
34. D. Gomez-Candon, A. I. De Castro, and F. Lopez-Granados, "Assessing the accuracy of mosaics from unmanned aerial vehicle (UAV) imagery for precision agriculture purposes in wheat," *Precis. Agric.* **15**, 44–56 (2014).
35. S. W. Ritchie, J. J. Hanway, and H. E. Thompson, "How a corn plant develops," Special Report 48, Cooperative Extension Service Ames, Iowa State University, Ames, Iowa (1996).
36. ESRI, "The mapping platform for your organization," ArcGIS, 2014, http://www.arcgis.com/features/index.html (29 July 2016).
37. Agisoft LLC, *AgiSoft PhotoScan User Manual; Professional Edition v.1.2.6*, Agisoft LLC, St. Petersburg, Russia (2016).
38. Exelis Visual Information Solutions, "ENVI 5.3.1," 2010, Exelis Visual Information Solutions, Boulder, Colorado, http://harrisgeospatial.com/ProductsandTechnology/Software/ENVI.aspx (4 August 2017).
39. S.A. Oyewole et al., "Classification of product images in different color models with customized kernel for support vector machine," in *IEEE Third Int. Conf. on Artificial Intelligence, Modelling and Simulation (AIMS)*, Kota Kinabalu, Malaysia, pp. 153–158 (2015).
40. C.-W. Hsu, C.-C. Chang, and C.-J. Lin, "A practical guide to support vector classification," 2016, Department of Computer Science National Taiwan University, Taiwan, http://ntu.csie.org/~cjlin/papers/guide/guide.pdf (1 December 2016).

41. H. Motulsky and A. Christopoulos, "Fitting models to biological data using linear and nonlinear regression," in *A Practical Guide to Curve Fitting* 2nd ed., GraphPad Software Inc., San Diego, California (2003).
42. H. Motulsky and R. E. Brown, "Detecting outliers when fitting data with nonlinear regression—a new method based on robust nonlinear regression and the false discovery rate," *BMC Bioinf.* **7**, 123 (2006).
43. D. I. Warton et al., "Smatr 3–an R package for estimation and inference about allometric lines," *Methods Ecol. Evol.* **3**, 257–259 (2012).
44. R Development Core Team, *R: A Language and Environment for Statistical Computing*, R Foundation for Statistical Computing, Vienna (2009).
45. K. J. Niklas, "A phyletic perspective on the allometry of plant biomass-partitioning patterns and functionally equivalent organ-categories," *New Phytol.* **171**, 27–40 (2006).
46. K. N. Tahar et al., "Assessment on ground control points in unmanned aerial system image processing for slope mapping studies," *Int. J. Sci. Eng. Res.* **3**, 1–10 (2012).
47. K. N. Tahar, "An evaluation on different number of ground control points in unmanned aerial vehicle photogrammetric block," in *Int. Archives of the Photogrammetry, Remote Sensing and Spatial Information Sciences, Volume XL-2/W2, ISPRS 8th 3DGeoInfo Conf. & WG II/2 Workshop*, Istanbul, Turkey, pp. 93–98 (2013).
48. M. Prajwal et al., "Optimal number of ground control points for a UAV based corridor mapping," *Int. J. Innovative Res. Sci. Eng. Technol.* **5**, 28–32 (2016).
49. I. A. Ciampitti, R. W. Elmore, and J. Lauer, *Corn Growth and Development*, Kansas State University Agricultural Experiment Station and Cooperative Extension Service, MF3305, Manhattan, Kansas (2016).
50. J. Geipel, J. Link, and W. Claupein, "Combined spectral and spatial modeling of corn yield based on aerial images and crop surface models acquired with an unmanned aircraft system," *Remote Sens.* **6**, 10335–10355 (2014).
51. N. Tilly et al., "Multitemporal crop surface models: accurate plant height measurement and biomass estimation with terrestrial laser scanning in paddy rice," *J. Appl. Remote Sens.* **8**, 083671 (2014).
52. L. K. Sharma et al., "Use of corn height measured with an acoustic sensor improves yield estimation with ground based active optical sensors," *Comput. Electron. Agric.* **124**, 254–262 (2016).
53. Y. Shi et al., "Unmanned aerial vehicles for high-throughput phenotyping and agronomic research," *PLoS One* **11**(7), e0159781 (2016).
54. E. Yin et al., "In-season prediction of corn yield using plant height under major production systems," *Agron. J.* **103**, 923–929 (2011).
55. L. Pordesimo, W. C. Edens, and S. Sokhansanj, "Distribution of above ground biomass in corn stover," *Biomass Bioenergy* **26**, 337–343 (2004).
56. T. J. Barten, "Evaluation and prediction of corn stover biomass and composition from commercially available corn hybrids," PhD Dissertation, Iowa State University, Ames, Iowa (2013).
57. O. Vergara-Diaz et al., "A novel remote sensing approach for prediction of maize yield under different conditions of nitrogen fertilization," *Front. Plant Sci.* **7**, 666 (2016).
58. H. Bach, "Yield estimation of corn based on multi-temporal Landsat-TM data as input for an agrometeorological model," *Pure Appl. Opt.* **7**, 809–825 (1998).

Sebastian Varela received his BS in soil science and agronomy from the University of the Republic, Uruguay. He is a Fulbright scholar and currently a PhD student in the Department of Agronomy at Kansas State University. His research focuses on multiscale crop forecasting using geographic information science and remote sensing.

Yared Assefa received his MS degree in statistics and PhD in agronomy from Kansas State University. He is currently a postdoctoral research associate in the Department of Agronomy at Kansas State University. He conducts quantitative and qualitative analysis in the area of crop production, plant physiology, soil fertility, and plant nutrition using statistical and GIS methods and tools.

P. V. Vara Prasad received his BS and MS degrees from Andhra Pradesh Agricultural University, India, and PhD from the University of Reading, UK. He is a university distinguished professor and director of the Sustainable Intensification Innovation Lab at Kansas State University. His research focuses on understanding crop responses to changing environments and management practices.

Nahuel R. Peralta received his PhD in soil science and agronomy from the faculty of agronomy, National University of Mar del Plata, Argentina. He was a director and advisor to numerous undergraduate and graduate theses. He is an author of numerous articles on precision agriculture, remote sensing, and soil science. He is currently a research and project management lead of Monsanto, South America.

Terry W. Griffin received his BS and MS degrees from the University of Arkansas and his PhD in agricultural economics from Purdue University in 2006. Currently, he is an assistant professor in the Department of Agricultural Economics. His research focuses on the adoption and profitability of precision agricultural technology and the valuation of farm data.

Ajay Sharda received his BS and MS degrees from Punjab Agricultural University, India, and his PhD in biosystems engineering from Auburn University in 2011. Currently, he is an assistant professor in the Department of Biological and Agricultural Engineering. His research focuses on the development, analysis, and experimental validation of control systems for agricultural machinery systems with special emphasis on sensing and automation; and developing thermal infrared imaging systems for crop health monitoring.

Allison Ferguson received her PhD in statistical physics from Brandeis University. She is the current director of research for PrecisionHawk, an unmanned aerial systems company focusing on the development of hardware and software solutions for UAS in a variety of commercial applications. She brings over 15 years of experience in the use of multivariate statistics and the development of predictive models to the PrecisionHawk team, with an emphasis on extracting actionable results in industrial applications.

Ignacio A. Ciampitti received his BS and MS degree from the University of Buenos Aires, Argentina, and his PhD in agronomy from Purdue University in 2012. Currently, he is an associate professor in the Department of Agronomy. His research focuses on the integration of crop production, plant physiology, and plant nutrition with remote sensing and modeling tools.